Doping effects on the phase separation in perovskite $La_{0.67-x}Bi_xCa_{0.33}MnO_3$

J. R. Sun,[1,2] J. Gao,[2] Y. Fei,[3] R. W. Li,[1] and B. G. Shen[1]

[1]*State Key Laboratory of Magnetism, Institute of Physics and Center for Condensed Matter Physics, Chinese Academy of Sciences, Beijing 100080, China*

[2]*Department of Physics, The University of Hong Kong, Pokfulam Road, Hong Kong*

[3]*Australian Nuclear Science and Technology Organization, Lucas Heights Laboratories, Menai 2234, Australia*

(Received 24 November 2001; revised manuscript received 15 July 2002; published 17 April 2003)

Effects of Bi, Cr, and Fe doping on phase separation of $La_{0.67}Ca_{0.33}MnO_3$ have been experimentally studied. As proved by the electron-spin resonance and neutron-diffraction studies, partial replacement of La by Bi causes the simultaneous occurrence of ferromagnetic (FM) phase and charge-ordered antiferromagnetic phase. As a consequence, two subsequent magnetic transitions at ~120 K and ~230 K are resulted. A strong coupling between the coexisted phases is assumed, which is responsible for the insensitivity of $T_c(L)$, the higher Curie temperature, to Bi doping after the appearance of phase separation, and consistent with the discontinuous variation of $T_c(L)$ with Cr doping. As expected, the substitution of Cr for Mn in this case promotes the FM order, but its effects are significantly different for the two magnetic states. Each Cr drives ~100 neighboring unit cells, for the high-moment state, and ~60 unit cells, for the low-moment state, into the FM state. Two definite processes can be identified for the melting of the charge-ordered phase. The FM fraction increases rapidly in the initial stage of Cr doping, and then slowly when the FM population exceeds ~90%. This could be a common feature of the phase-separated system suffering from random-phase fluctuation according to a theoretical analysis. Exactly opposite effects on phase constituent are produced by Cr doping and Bi doping, and 1% Cr are equivalent to ~4.6% Bi. In contrast, both Cr doping and magnetic field promote the FM order. 1% Cr correspond to a field of ~4.5 T for the low-moment state and 6 T for the high-moment state, reducing the energy difference between the charge ordering and the FM states by ~0.96 meV/Mn and ~1.3 meV/Mn, respectively.

DOI: 10.1103/PhysRevB.67.144414 PACS number(s): 75.50.Dd, 75.47.Gk, 72.80.−r

I. INTRODUCTION

The magnetoresistance (MR) effect of manganese oxides has been a focus of scientists in recent years. The rich physics and potential application of this effect are the reason for that it is world widely interested.[1] In these kind of materials, in addition to the extremely large MR effect, the crystal structure, magnetic structure, and electronic structure couple to each other strongly, and can vary in a wide range with the concentration of doped holes or lattice distortions.[2–4] One of the most striking features of the manganites may be the charge and orbital ordering,[5–7] that is, under proper conditions an ordering of the spatial arrangement and the orbital orientation of the e_g electron takes place. Typical charge ordering (CO) occurs in the half-hole-doped manganites such as $La_{0.5}Ca_{0.5}MnO_3$ (Ref. 8) and $Nd_{0.5}Sr_{0.5}MnO_3$,[9] leading to two subsequent magnetic transitions: a paramagnetic (PM) to ferromagnetic (FM) transition followed by a ferromagnetic to antiferromagnetic (AFM) transition. There are also compounds such as $Pr_{1-x}Ca_xMnO_3$ ($x>0.3$) (Ref. 10) and $La_{1-x}Ca_xMnO_3$ ($x>0.5$),[11] in which CO develops well above the AFM transition. Considering the partiality of double exchange (DE) for charge transferring,[12,13] which is believed to be responsible for the magnetic coupling between Mn ions, a strong competition between the CO and DE is expected. As a consequence, the behavior of the compound can be complicated greatly for that any external disturbance influencing the instable balance could produce dramatic effects. This competition was indeed observed in many compounds, and $La_{0.67-x}Nd_xCa_{0.33}MnO_3$ ($x=0.33$), among them, is one of the most interesting examples.[14] A remarkable behavior of $La_{0.67-x}Nd_xCa_{0.33}MnO_3$ is the stepwise magnetization. When cooled, the system undergoes an ordinary PM to FM transition first. Further cooling produces minor effects until a critical temperature, at which a second jump in magnetization appears. This feature remains for further doping though the overall magnetization reduces significantly. Rao and co-authors[14] explain this behavior in a scenario of the coexistence of La-rich and Nd-rich domains in the compounds. Though the presence of chemical segregation was not confirmed, subsequent studies revealed the occurrence of charge-ordered phase,[15] which suffers from an AFM to FM spin rearrangement under magnetic field. Different from the half-hole-doped manganites mentioned above, the emergence of the CO in $La_{0.67-x}Nd_xCa_{0.33}MnO_3$ is unable to depress the FM ordering completely. On the contrary, the magnetization even shows a tendency to enhancement with cooling, resulting in a two-step magnetic behavior. The coexistence of more than one phase of different character and their competitive instability are believed to be the origin of the extremely large MR effects[16] and the amazing thermal and magnetic history dependent behaviors observed.[17] Unfortunately, this kind of phase separation did not receive deserved attention until the work by Uehara *et al.*[18] for a similar system $La_{0.625-x}Pr_xCa_{0.375}MnO_3$.

The phase constituent of the two magnetic states, its evolution, and the coupling between phases may be basically important for the understanding of the complex behavior associated with phase separation. A recent attempt was the work by Kiryukhin and co-workers,[19] in which the

evolution of the CO phase with temperature in $La_{0.275}Pr_{0.35}Ca_{0.375}MnO_3$ was investigated by means of synchron x-ray diffraction. This work suggested the presence of charge-disordered PM phase in the high-temperature magnetic state. Based on an impedance measurement, however, Souza *et al.*[20] argued that two phases, both undergo a metal to insulator transition, existed in $La_{0.3}Pr_{0.4}Ca_{0.3}MnO_3$. In a similar compound $Pr_{0.7}Ca_{0.3}MnO_3$, a signature of complex orbital ordering, in addition to the ordinary charge and orbital ordering, was further reported.[21]

The disagreement between the results of different groups indicates that, though the intensive studies, we are still far away from a thorough understanding of the phase-separated system. Therefore, a comprehensive investigation on, for example, how and when the two-step magnetic behavior takes place, the evolution of the phase constituent, and related effects is no doubt necessary. Mn-site doping has been proved powerful to affect the double exchange and CO competition. The presence of Cr ion at Mn site can destroy the CO completely,[22] while Fe ions depress the FM order.[23] What their effects will be when two competitive phases coexist, and how the two magnetic transitions, which are believed to be different in nature, vary when the secondary atoms are introduced into the Mn sites, these are the topics of the present paper. By replacing La with Bi in $La_{0.67}Ca_{0.33}MnO_3$, we first rebuilt the stepwise behavior, then introduced Cr or Fe into Mn site in an attempt to tune the proportion of coexisted phases and affect the coupling between phases. Effects thus resulted were studied experimentally. The layout of this paper is as follows: the following section is a simple description of the experiment procedure. Section III presents the main results: crystal structure, stepwise magnetic behavior, phase constituent, and its evolution under the Cr/Fe doping or external magnetic field. A qualitative theoretical analysis on the experiment results and corresponding discussions are given in Sec. IV. The last section is a brief summary.

II. EXPERIMENT

Polycrystalline samples $La_{0.67-x}Bi_xCa_{0.33}MnO_3$ ($x=0.067$, 0.083, 0.1, 0.117, 0.133, 0.15, 0.167, 0.18, 0.193, and 0.2), $La_{0.474}Bi_{0.193}Ca_{0.33}Mn_{1-y}Cr_yO_3$ ($y=0.003$, 0.0045, 0.006, 0.009, and 0.014), and $La_{0.52}Bi_{0.15}Ca_{0.33}Mn_{1-z}Fe_zO_3$ ($z=0.01$, 0.02, and 0.03) were prepared by the conventional solid-state reaction method. Well mixed stoichiometric amount of the La_2O_3, Bi_2O_3, $CaCO_3$, Cr_2O_3 (Fe_2O_3), and MnO_2 powders were calcinated at 1000 °C for 24 hr first. The resulting products were then ground, pelletized, and sintered at 1250 °C for 72 hr with an intermediate grinding for homogenization.

Considering the strong tendency of $Bi_{1-x}Ca_xMnO_3$ to CO,[24] Bi, instead of the frequently used Nd or Pr, was chosen to replace La in $La_{0.67}Ca_{0.33}MnO_3$. Cr doping was carried out for the compound with a high Bi content ($x=0.193$), in which the CO phase may be the dominant phase. In contrast, a low Bi-content (0.15) compound was chosen for Fe doping considering the depression of the FM order by Fe.

Phase purity and crystal structure of the synthesized samples were examined by powder x-ray diffraction using a Rigaku x-ray diffractometer with a rotating anode and Cu Kα radiation. Neutron diffraction was conducted on a Medium Resolution Powder Diffractometer at the Australian Nuclear Science and Technology Organization (ANSTO) for selected temperatures between 5 K and 300 K. Electron-spin-resonance (ESR) spectra in the range 120–290 K were measured by a Bruker ER-200D spectrometer operated at a frequency of 9.5 GHz. A quantum design magnetometer (SQUID) was used for the magnetic measurements. All the data presented here were collected in the warming process.

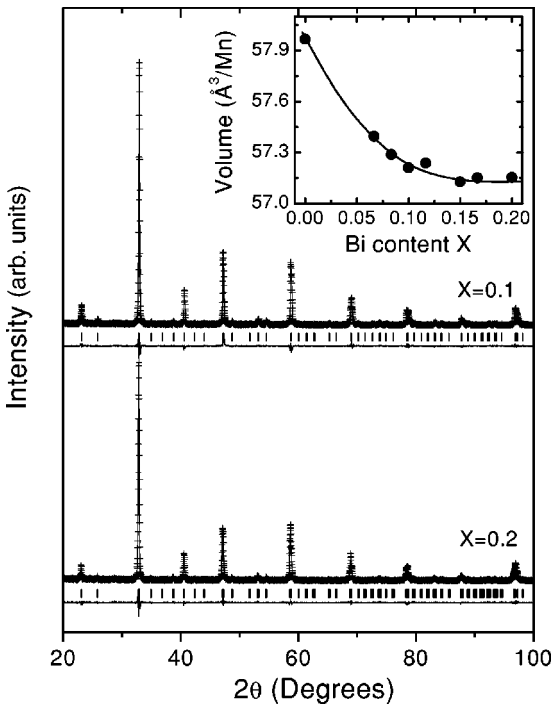

FIG. 1. Room-temperature x-ray-diffraction patterns of $La_{0.67-x}Bi_xCa_{0.33}MnO_3$ for selected $x=0.1$ and 0.2. Differences between the observed (crosses) and calculated (solid line) results are shown in the bottom of the figure with a downward shift for clarity. Vertical bars represent the positions of the Bragg reflections. The reliability of the Rietveld refinement are $R_p=11.3\%$, $R_{wp}=17.0\%$, and $S=1.19$ for $x=0.1$ and $R_p=11.7\%$, $R_{wp}=16.1\%$, $S=1.21$ for $x=0.2$. Inset, cell volume as a function of the content of Bi. Solid line is a guide for the eye.

III. RESULTS

A. Crystal structure

All the samples are of single phase as confirmed by the excellent agreement of the measured and calculated (Rietveld refinement[25] based on the space group *Pnma*) x-ray-diffraction spectra (Fig. 1). The incorporation of smaller Bi causes a monotonic decrease of the volume of unit cell while the structure symmetry remains unaffected, which is also a general feature of the rare-earth-doped $La_{0.67}Ca_{0.33}MnO_3$.[14,26]

B. Stepwise magnetization produced by Bi doping

Magnetization (M) of $La_{0.67-x}Bi_xCa_{0.33}MnO_3$ as a function of temperature was measured. The applied field was so

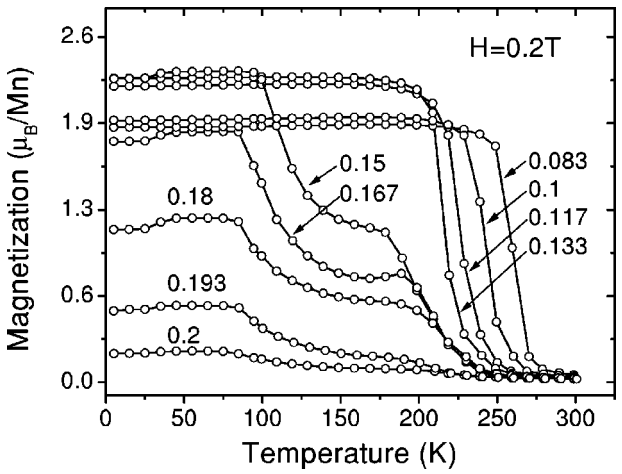

FIG. 2. Temperature-dependent magnetization of $La_{0.67-x}Bi_xCa_{0.33}MnO_3$ measured under a field of 0.2 T. Two magnetic states appear for $x \geqslant 0.14$.

chosen that it saturates the sample but not affects its magnetic structure. Figure 2 presents the thermal magnetization under a field of 0.2 T. It shows a steady decrease of the Curie temperature (T_c) with *x*, the content of Bi. An abrupt change in the $M(T)$ relation is observed when *x* exceeds 0.133: the magnetization in the high-temperature region decreases drastically, resulting in a stepwise behavior. As a consequence, the single T_c splits into two values of $\sim$120 K and $\sim$230 K. This feature remains for further doping.

Figure 3 depicts the Curie temperature as a function of *x*, where $T_c(L)$ and $T_c(H)$ correspond to the low-moment state (LMS) and the high-moment state (HMS), respectively, and their definition is illustrated in the inset of Fig. 3. The linear decrease of $T_c(H)$ in the beginning of the doping is simply a

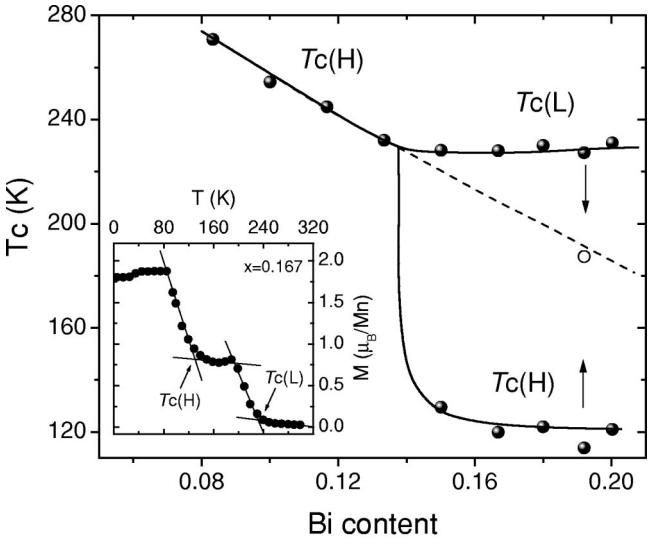

FIG. 3. Critical temperature for magnetic transition as a function of doping level. $T_c(L)$ and $T_c(H)$ correspond to the low-moment state (LMS) and the high-moment state (HMS), respectively. The dashed line shows the expected results without phase separation. White circles represent the drop of $T_c(L)$ after proper Cr doping. The inset demonstrates the definition of $T_c(L)$ and $T_c(H)$.

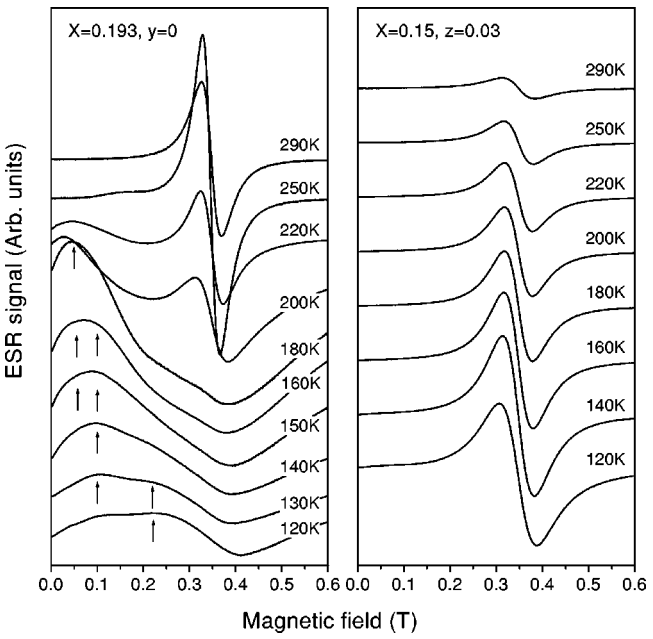

FIG. 4. Electron-spin-resonance (ESR) spectra at different temperatures for $La_{0.474}Bi_{0.193}Ca_{0.33}MnO_3$ (left panel) and $La_{0.52}Bi_{0.15}Ca_{0.33}Mn_{0.97}Fe_{0.03}O_3$ (right panel). The frequency of the microwave is 9.5 GHz. Arrows mark the maximum of the derivative FM resonance peak.

consequence of enhanced lattice distortions due to the introduction of smaller Bi.[3] A new magnetic process marked by the sharp drop of $T_c(H)$ takes place at $x \simeq 0.14$. After that, the Curie temperatures of the HMS and LMS keep essentially constant for further doping. These are prototypical behaviors observed previously by Rao *et al.*[14] in $La_{0.67-x}Nd_xCa_{0.33}MnO_3$ and Uehara *et al.*,[18] and Kim *et al.*[27] in $La_{0.625-x}Pr_xCa_{0.375}MnO_3$. Even the values of the $Tc(L)$ and $Tc(H)$ are very similar for the three series. However, compared with the above two compounds, the threshold doping for the occurrence of the two-step magnetization in the present system is much lower ($x \sim 0.2$ for $La_{0.67-x}Nd_xCa_{0.33}MnO_3$ and $\sim$0.25 for $La_{0.625-x}Pr_xCa_{0.375}MnO_3$).

C. Phase constituent of the two magnetic states

To examine the phase constituent, the ESR spectra of $La_{0.474}Bi_{0.193}Ca_{0.33}MnO_3$ were measured, and the results are shown in Fig. 4 (left panel). Above 250 K, the PM phase is the only detectable phase, which contributes a single Lorentzian line at $H = 0.35$ T ($g = 2.0$). FM phase sets in at $\sim$250 K, marked by the appearance of a hump in the low-field region, and its population increases with cooling. As a consequence, the PM signal decreases progressively and, finally, becomes invisible. To get a quantitative description for the coexisted phases, the integrated ESR spectra have been fitted to the Lorentzian functions with adjustable resonance field, linewidth, and intensity, and the typical results are shown in Fig. 5. Two absorption lines centered at two fields LF and HF, respectively, have to be used to reproduce the spectra between 160 K and 250 K. LF takes $\sim$0.15 T be-

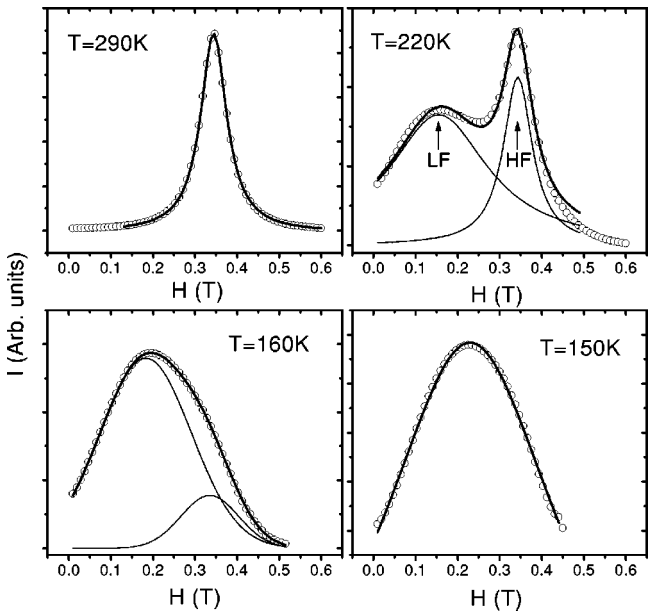

FIG. 5. Integrated electron-spin-resonance spectra at selected temperature $T=290$ K, 220 K, 160 K, and 150 K, respectively. Solid lines are fitting based on the Lorentizan functions. Two resonance lines are required in the case $T=220$ K and 160 K. LF and HF denote the resonance fields of the PM and the FM phases, respectively.

tween 160 K and 220 K, whereas HF decreases from ~ 0.35 T to ~ 0.3 T when the temperature changes from 250 K to 160 K. Obviously, the two resonance fields correspond to the contributions from the FM and the PM phases, respectively (the slight decrease of HF is an effect of the small internal field from the FM region[28]). The percentage of the PM phase is proportional to the area of the resonance peak at HF. A direct calculation shows that the relative area of the PM line decreases from $\sim 100\%$ for $T=250$ K to $\sim 15\%$ for $T=160$ K, and only a singlet with LF $\simeq 0.2$ T is required to fit the spectra at $T=150$ K.

Corresponding to the simple magnetic transition in the temperature region from 100 K to 140 K (Fig. 2), ESR study reveals a much complex process. Further cooling below 140 K produces an evolution of the phases. A new phase with higher resonance field first develops near ~ 140 K, and it is replaced gradually by another phase with an even high resonance field (~ 0.22 T) at ~ 120 K. The complex variation of resonance field could be a sign of the rearrangement of spin orientation and domain structure near $Tc(H)$ noting a fact that the resonance field is a combined result of demagnetization field, anisotropic field, and internal field of the FM phase. Marking the maximum of the ESR signal by arrows, the systematic from 160 K to 120 K is obvious. These seem to be the common features of the phase-separated system for that similar behaviors are also observed in $La_{0.503}Bi_{0.167}Ca_{0.33}MnO_3$ (not shown) though the PM population of the LMS and the HMS, and the magnetization increase at $Tc(H)$ are different for both compounds.

To get further information on the AFM structure and the CO transition, neutron diffraction was subsequently performed for the sample $x=0.193$ ($\lambda=1.66$ Å). Only the

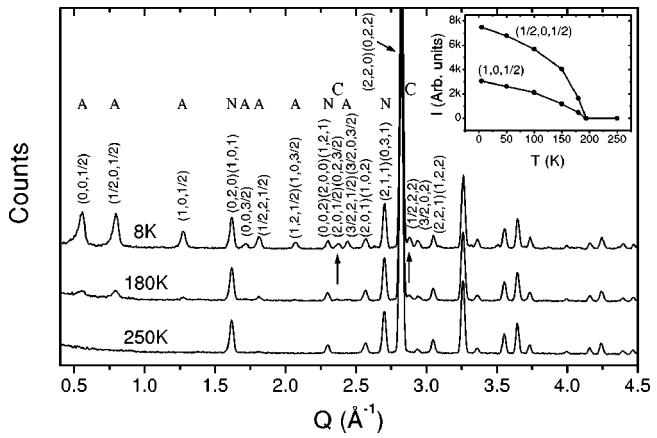

FIG. 6. Neutron-diffraction patterns for $La_{0.474}Bi_{0.193}Ca_{0.33}MnO_3$ at selected temperature 8 K, 180 K, and 250 K ($\lambda=1.66$ Å). Only the main peaks are indexed, and the peaks corresponding to the nuclear reflections are marked by *N*, to the AFM reflections by *A*. Two reflections corresponding to the charge and orbital ordering are marked by *C*. The inset is a plot showing the variation of the integrated intensity of the (1/2,0,1/2) and (1,0,1/2) peaks.

nuclear reflections are observed above 250 K (labeled by *N*). When the sample is cooled below 180 K, additional peaks that can be indexed based on an AFM superlattice appear. Particularly, the appearance of the characteristic peaks for the CO and orbital ordering structure (labeled by *C*) indicates that the sample is CE-type AFM at low temperature. (According to Yoshizawa *et al.*[29] and Kiryukhin *et al.*,[19] the $(h,k,l/2)$ peaks, l odd, are associated with the Jahn-Teller distortions characteristic of the CE-type charge and orbitally ordered state). This feature remains down to 8 K, the lowest temperature of this experiment. In Fig. 6 we show three selected powder patterns collected at 8 K, 180 K, and 250 K, respectively. The inset is a plot showing the variation of the integrated intensity of the peaks (1/2,0,1/2) and (1,0,1/2) against temperature.

Combining the results of magnetic, ESR, and neutron-diffraction measurements, it is clear that the PM phase dominates above 250 K, PM and FM phases coexist between 250 K and 160 K (the population of the former decrease rapidly with cooling). Charge-ordered AFM phase appears at ~ 180 K, and coexists with the FM phase down to the lowest temperature of the present experiment.

The right panel of Fig. 4 displays the ESR spectra of $La_{0.52}Bi_{0.15}Ca_{0.33}Mn_{0.97}Fe_{0.03}O_3$. As expected, the introduction of Fe suppresses the FM order greatly, and only the PM spectra are detected down to 120 K. The analysis of the peak width indicates an abnormal change at ~ 160 K (not shown), however, the main features of the resonance remain PM.

D. Variation of phase constituent with Cr or Fe doping

If more than one phase exist in the manganites, we can affect their proportions via replacing Mn with Cr or Fe, and estimate their volume fractions based on magnetic measurements. Figure 7 shows the isothermal magnetization against applied field (H) for $La_{0.474}Bi_{0.193}Ca_{0.33}Mn_{1-y}Cr_yO_3$. Re-

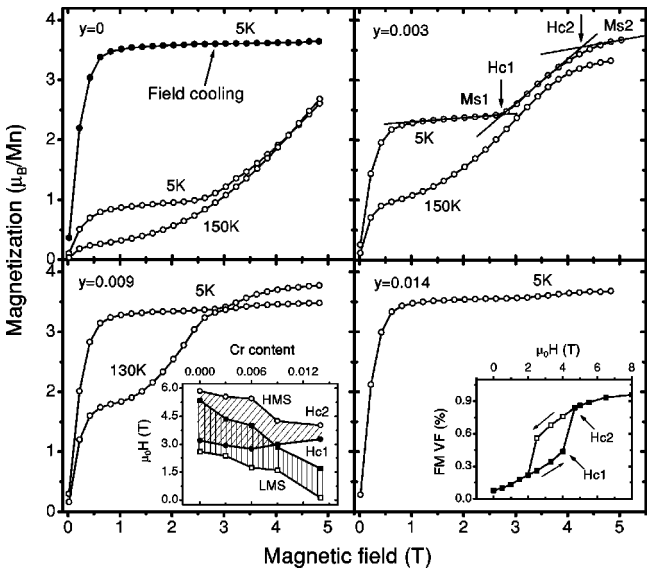

FIG. 7. Isothermal magnetization of $La_{0.474}Bi_{0.193}Ca_{0.33}Mn_{1-y}Cr_yO_3$ measured at 5 K, 130 K, and 150 K, respectively. Results represented by black circles were obtained by cooling the sample in the presence of a field of 5 T. The lower left inset displays the Cr-content dependence of the critical field for the onset (H_{c1}) and the end (H_{c2}) of the CO collapse. The lower right inset are calculated results demonstrating the melting of the charge-ordered phase under magnetic field. M_{s1} and M_{s2} denote the saturation magnetization before and after the CO collapse. HMS and LMS represent the high-moment and low-moment states, respectively. Solid lines are guides for the eye.

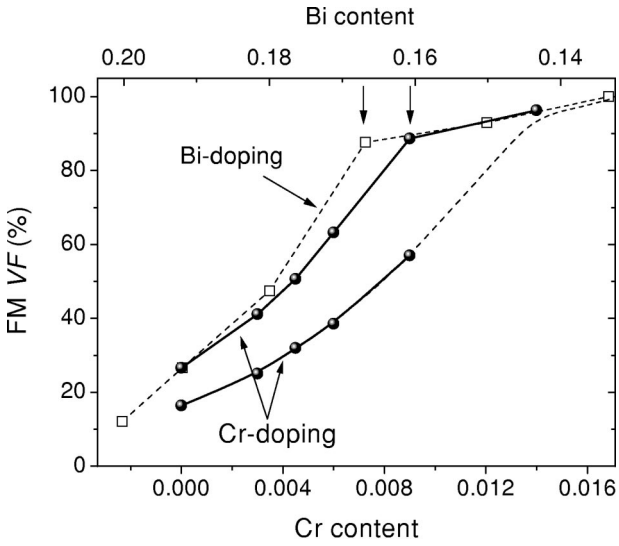

FIG. 8. Volume fraction of the FM phase as a function of the content of Bi/Cr. LMS and HMS represent the low-moment state and the high-moment state, respectively. Arrow in the figure marks the kink that leads to a VF saturation. Solid and dashed lines are guides for the eye.

sults at $T=5$ K correspond to the HMS, while those at $T=150$ K to the LMS. The saturation temperature of the LMS is set to 130 K for $y=0.009$ taking into account the decrease of $Tc(L)$ (*vide infra*). As expected, the magnetization increases with H rapidly, and the first saturation is obtained at $H\sim 0.5$ T. Further increase in magnetic field produces minor effects until a critical field H_{c1}, at which a significant magnetization enhancement appears: the CE-type AFM phase is unstable under magnetic field, and converts into the FM phase. The second saturation is reached at a higher field (H_{c2}) depending on sample, typically ~ 5 T. Without Cr doping, a full alignment of the core spins of the Mn ions requires much higher fields (>6 T). To obtain the magnetic saturation, in this case we cooled the sample under a magnetic field of 5 T, which causes an overcooling of the FM order. The lower left inset of Fig. 7 demonstrates the variation of H_{c1} and H_{c2} vs y. The H_{c2} value corresponding to $y=0$ is obtained by a simple extrapolation of the results in the upper left panel.

The FM volume fraction in the compound can be calculated via $VF=M_{s1}/M_{s2}$, where M_{s1} and M_{s2} are the saturation magnetizations before and after the CO collapse (Fig. 7). Results thus obtained are presented in Fig. 8. Without Cr doping, the dominant phase is the charge-ordered phase, and the FM phase occupies only $\sim 27\%$ and $\sim 16\%$ of the total for the HMS and the LMS, respectively. VF increases monotonically with the increase of the content of Cr, revealing a partial melting of the CO phase. The curvature of the *VF-y* curve is a sign of strong correlations between FM domains. The average VF-y slope is ~ 7000/Cr for $y\leqslant 0.009$, which means that each Cr drives ~ 100 neighboring cells into the FM state. However, it appears that the efficiency of Cr decreases when the FM fraction is high, and the VF-y slope reduces to ~ 1500/Cr after an obvious kink at $y=0.009$ (where VF$\simeq 88\%$). This is a value similar to ~ 1600/Cr observed in the Cr-doped $Nd_{0.5}Ca_{0.5}MnO_3$ by Kimura *et al.*[30] For the LMS, the FM VF is only calculated for $y\leqslant 0.009$ because of the ambiguousness of the stepwise behavior in the specimen $y=0.014$. It should vary along the thin line for $y>0.009$ by a smooth extrapolation of the low y values and a comparison with the results under magnetic fields (see the context). A simple calculation gives the average VF-y slope of ~ 5700/Cr for the LMS (~ 60 unit cells are affected by each Cr ion). It is obvious that the efficiency of Cr to melt the CO phase is significantly different for the HMS and LMS.

One of the most striking observations of the present work is the stepwise melting of the CO phase with the incorporation of Cr. The volume fraction of the FM phase grows rapidly with the increase of the content of Cr until $y=0.009$ (VF$\sim 88\%$). After that, the efficiency of the Cr doping weakens significantly. Similar behavior is also observed in the case of Bi doping (dashed lines in Fig. 8). This could be a common feature of the phase-separated system suffering from phase fluctuation as discussed later.

Different from Cr doping, the incorporation of Fe depresses the FM order, which can be observed from either the ESR or the magnetic measurements. Figure 9 exemplifies a gradual decrease of the saturation magnetization at 5 K ($Ms2$) with the content of Fe in $La_{0.52}Bi_{0.15}Ca_{0.33}Mn_{1-z}Fe_zO_3$. The dashed line is a calculation assuming an AFM coupling between Fe and host Mn. Obviously, Fe does not influence the magnetic order except

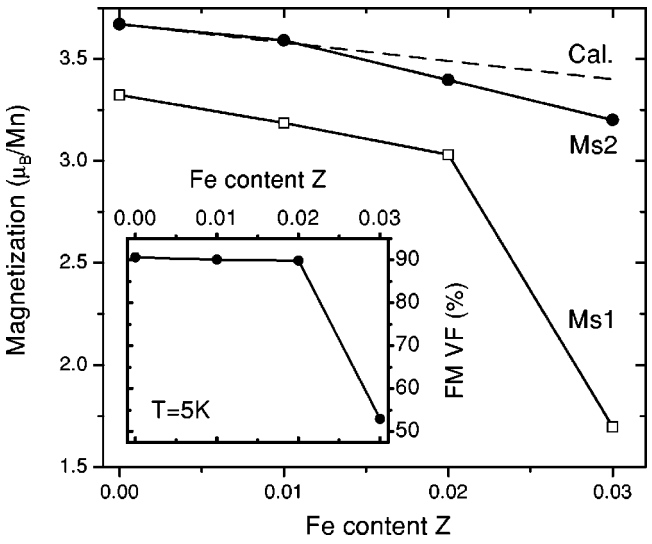

FIG. 9. Magnetic moment of the Mn ions before (M_{s1}) and after (M_{s2}) the change of magnetic structure for $La_{0.52}Bi_{0.15}Ca_{0.33}Mn_{1-z}Fe_zO_3$. Dashed line is a theoretical prediction of the saturation magnetization assuming an AFM coupling between Fe and host Mn. Inset is a plot showing the FM volume fraction in the compounds. Solid lines are guides for the eye.

for diluting the Mn ions for $z \leqslant 0.02$. However, the magnetic fraction drops suddenly from ~90% to ~50% at $z=0.03$ (inset to Fig. 9), indicating a fact that large number of Fe will influence the FM order of the phase-separated compounds strongly. The remaining phases can be either charge ordered AFM or PM phase. An estimate of their respective volume fraction is unable based on the present data.

E. Variation of T_c with Cr or Fe doping

It is generally believed that the two magnetic transitions at $T_c(L)$ and $T_c(H)$ are different in nature. The former inherits all the characters of an ordinary PM-FM transition, while the latter is a result of the percolation of magnetic phase in the CO background.[19] It would be interesting to examine the behavior of $T_c(L)$ and $T_c(H)$ under the Cr and Fe doping. Figure 10 presents the thermal magnetization of $La_{0.474}Bi_{0.193}Ca_{0.33}Mn_{1-y}Cr_yO_3$. A direct consequence of the incorporation of Cr is the depression of the two-step magnetization: the stepwise behavior is clear for $y \leqslant 0.006$, weak but identifiable for $y=0.009$, and completely invisible for $y=0.014$. This behavior is relevant to the variation of phase constituent, but the apparent reason is the variation of $T_c(L)$ and $T_c(H)$. The inset in Fig. 10 illustrates the effects of Cr doping on the two Curie temperatures. It shows a linear decrease of $T_c(L)$ at a rate of ~7 K per 1% Cr for $y \leqslant 0.006$. This could be an ordinary doping effect noting a fact that the modest change of T_c is ~8 K for $La_{0.7}Ca_{0.3}MnO_3$ when 1% Mn is replaced by Cr.[31] It is a consequence of the impediment of the double exchange process by Cr, and the effects associated with the reduction of the CO fraction are not obvious at this stage. When y exceeds 0.006, however, an abrupt drop of $T_c(L)$ from ~220 K to ~185 K takes place. It is interesting to note that $T_c(L) \approx 185$ K for $y=0.009$ is

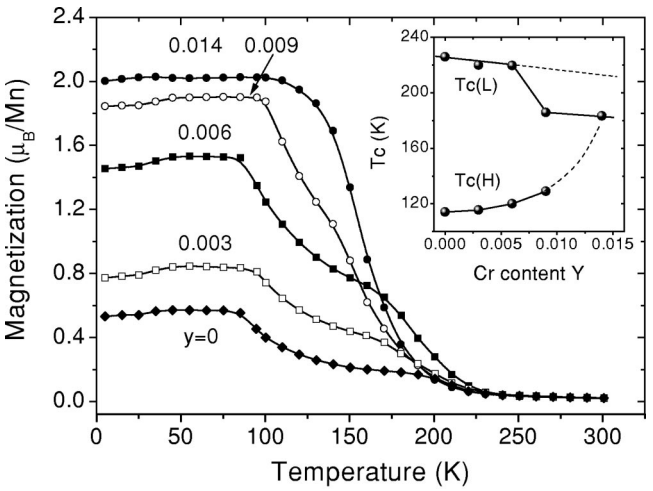

FIG. 10. Thermal magnetization of $La_{0.474}Bi_{0.193}Ca_{0.33}Mn_{1-y}Cr_yO_3$ measured under a field of 0.2 T. Stepwise behavior fades away gradually with the incorporation of Cr. The inset is a plot of $T_c(L)$ and $T_c(H)$ against the content of Cr. Dashed lines denote the assumed $T_c(L)$.

approximately the value predicted by lattice effects (~190 K), and the ~5 K lower of the former could be a result of the presence of Cr ions, which, in addition to melting the CO phase, depress the magnetic coupling in the FM phase.[31] Therefore, the discontinuous variation of $T_c(L)$ may indicate a sudden return to the conventional lattice effects at a critical doping level. In contrast, $T_c(H)$ increases slowly and smoothly with y, and a simple estimate gives the average temperature change of ~12 K per 1% Cr.

When Fe is introduced into $La_{0.52}Bi_{0.15}Ca_{0.33}MnO_3$, we observed a decrease of $T_c(L)$ of ~23 K per 1% Fe (Fig. 11) for $z \leqslant 0.02$. This is a rate similar to that observed in the Fe-doped $La_{0.7}Ca_{0.3}MnO_3$ (~22 K per 1% Fe),[23] which indicates that the FM phase behaves as an ordinary FM phase in spite of the presence of other phases. When z exceeds

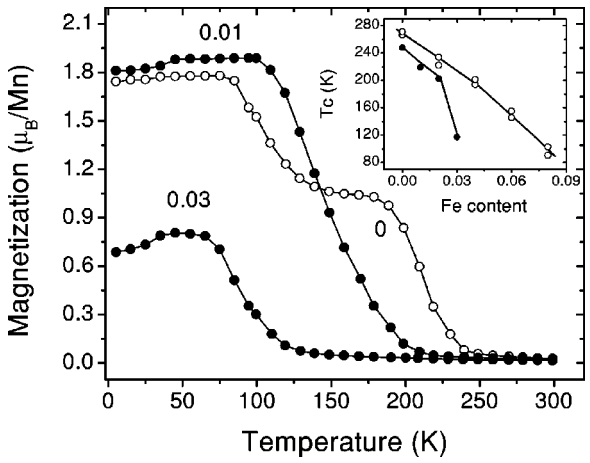

FIG. 11. Temperature-dependent magnetization of $La_{0.52}Bi_{0.15}Ca_{0.33}Mn_{1-z}Fe_zO_3$ measured under a field of 0.2 T. The inset displays the Curie temperature as a function of the content of Fe: black symbols for $La_{0.52}Bi_{0.15}Ca_{0.33}Mn_{1-z}Fe_zO_3$ and white symbols for $La_{0.7}Ca_{0.3}Mn_{1-x}Fe_xO_3$.

0.02, however, $T_c(L)$ drops rapidly ($\sim$85 K per 1% Fe). This is in sharp contrast to $La_{0.7}Ca_{0.3}MnO_3$, for which the Curie temperature decreases smoothly with the content of Fe until $z=0.1$, and there is no discontinuous change. This effect can be ascribed to the coexisted CO phase, which depresses the FM order when the instable balance between the FM and AFM phases is disturbed by the incorporation of Fe. Fe also affects the second magnetic transition. Fascinatingly, $T_c(H)$ exhibits an enhancement with Fe doping for $z=0.01$ and 0.02, which indicates that this is not a simple PM-FM transition considering a fact that the presence of Fe disfavors the FM order.

IV. DISCUSSIONS

(i) Stepwise magnetic behavior is only reported in Nd- or Pr-doped manganites before. Observation of this behavior in the Bi-doped compounds reveals the generality of this kind of phase separation. Based on the present study, we expect its appearance when appropriate amount of La in $La_{1-x}Ca_xMnO_3$ ($x=0.33$-0.4) are replaced by atom A that shows a tendency to CO, which can be measured by, for example, the T_{CO} of $A_{0.5}Ca_{0.5}MnO_3$, and the threshold doping level (x_c) depends on A. It seems that the stronger the tendency is, the smaller the threshold doping will be. For instance, T_{CO} is $\sim$240 K, $\sim$250 K and $\sim$315 K, respectively, for $Nd_{1/2}Ca_{1/2}MnO_3$, $Pr_{1/2}Ca_{1/2}MnO_3$, and $Bi_{1/2}Ca_{1/2}MnO_3$, and the corresponding x_c is $\sim$0.25,[27] $\sim$0.2 (Ref. 14) and $\sim$0.14.

(ii) Our results without Cr/Fe doping are compatible with those obtained by Uehara *et al.*[18] and Kim *et al.*[27] for $La_{0.625-x}Pr_xCa_{0.375}MnO_3$ in that phase separation takes place after a threshold doping, and it leads to two subsequent magnetic transitions at two Curie temperatures insensitive to the content of the dopants. In another system $Pr_{0.65}Ca_{0.35-x}Sr_xMnO_3$, however, Niebieskikwiat and coauthors reported a slight but visible decrease of the Curie temperature with lattice distortion even when the phase separation occurred.[32] It is worth noting that a different parameter (T_S) was used in their work, which is defined as the inflection point of the ln(M)-T curve, and may correspond to the onset of short-range FM order. In fact, a sign of local FM correlation is also shown in our samples $x=0.167$ and 0.193, exhibited as a cusp in the low-field side of the PM signal in the ESR spectra at 250 K. This agrees with that $T_S\sim$250 K observed by Niebieskikwiat *et al.* in $Pr_{0.65}Ca_{0.25}Sr_{0.1}MnO_3$.

The nature of the low-temperature transition is an issue in debating. It has been naturally ascribed to a CO-FM transition since the discovery of the presence of the CO phase. The first suspicion about this explanation comes from Kiryukhin *et al*[19] after the failure to detect the variation of the CO phase across $T_c(H)$ by synchron x-ray diffraction. Though the work of Niebieskikwiat *et al.* on $Pr_{0.65}Ca_{0.35-x}Sr_xMnO_3$ is rather comprehensive, the main techniques utilized there are magnetic and resistive measurements, for which it is somewhat difficult to distinguish the CO-FM transition from the PM-FM transition. We hope the neutron diffraction and ESR techniques can provide us further information on the process of phase separation considering their respective sensitivity to the AFM and PM phases. One of the most striking results of the present work is the absence of the PM phase below 160 K. According to Fig. 8, the FM fraction increases from $\sim$16.4% to $\sim$26.6% for the sample $x=0.193$ when the system transits from the LMS to the HMS, which implies that the PM component, if exists, could be $\sim$10% of the total based on a rough estimate. Considering the enhancement of the PM resonance at low temperatures, the PM phase should be visible for the ESR technique. With this in mind, the disappearance of the PM signal in the low-temperature region indicates that the magnetic jump in our samples may not be a simple PM-FM transition.

We further studied the neutron-diffraction spectra carefully, and found a smooth increase of the integrated intensity of the (1/2,0,1/2) peak (it corresponds to the contribution of the AFM phase) with cooling (inset in Fig. 6). The absence of any anomalies around $T_c(H)$ indicates that the low-temperature transition may not be a CO AFM-FM transition either.

We also studied the structure of $La_{0.67-x}Bi_xCa_{0.33}MnO_3$ ($x=0.167$) as a function of temperature. A sudden change of the lattice parameters from $a=5.456$ Å, $b=5.450$ Å, and $c/\sqrt{2}=5.436$ Å to $a=5.466$ Å, $b=5.451$ Å, and $c/\sqrt{2}=5.422$ Å is observed when the sample is cooled through $T_c(L)=220$ K (not shown). a and b increase whereas c decreases, which is a typical feature of the systems undergoing a CO transition.[33] The relative change of c is $\sim$0.3% around $T_c(L)$, and the difference between a and c is $\sim$0.8%. Considering the coexistence of the FM and CO phases below $T_c(L)$ in this compound and a fact that the structure variation of the former is negligibly small, the actual lattice change of the CO phase may be even large. In fact, we have found a reduction of $\sim$0.9% of c in $Bi_{0.5}Ca_{0.5}MnO_3$ around the CO temperature (not shown). It is easy to image that if an FM domain and a CO domain or two CO domains with different orientations appear in the same grain, considerable strains would occur near the FM-CO or the CO-CO interface, resulting in a behavior deviating from that of the bulk. The appearance of the martensitic accommodation strain in the CO phase reveals the importance of the elastic energy associated with the strains.[34] In fact, a lattice mismatch of 0.5–0.7% may be enough to modify the behavior of the interfacial phase. It is found that the CO phase of the $Pr_{0.5}Ca_{0.5}MnO_3$ film on (100)-$LaAlO_3$ (thickness 1100 Å), for which the film-substrate lattice mismatch is $\sim$0.7%, is much more unstable compared with the bulk material: its melting field reduces from 20 T to 5 T.[35–37] Meanwhile, the satellite peaks corresponding to the CO structure become weak and diffusive, and no lattice images with the CO modulation can be obtained. All these can be attributed to the effects of strains, which prevents the full development of the lattice distortions accompanying the CO transition. Actually, there is a report that the underlying substrate can fix the lattice of the film, thus depress the CO transition.[38] On analogy, the CO in strained regions of the phase-separated compound may be imperfect, and possibly only charge-ordered fragments are formed, which could be the reason for that the neutron or synchron x-ray diffraction failed to capture them effectively. With the decrease of temperature, the short range CO phase

becomes unstable, and transits into the FM phase, while due to the distribution of structure relaxation the magnetic transition is diffusive and of percolation origin in nature. The interfacial phase is nodoubt an important factor affecting the magnetic behavior of the manganites. Recently, Mahendiran *et al.* studied the effects of thermal history in $Pr_{0.5}Ca_{0.5}Mn_{0.985}Cr_{0.015}O_3$, and found that the magnetization decreased by ~35% after repeated thermal cycling, while the electron diffraction and the x-ray diffraction indicate no obvious change in the CO structure.[39] The authors have ascribed these observations to the change of the magnetic order in interfacial regions.

According to Prellier *et al.*, significant lattice relaxation exists even when the thickness of the $Pr_{0.5}Ca_{0.5}MnO_3$ film exceeds 1000 Å.[36] This may be a special case. However, in any case a structure relaxation within 200–400 Å is expected for the manganite films.[40] Though the lattice mismatch between different phases in our samples could be somewhat smaller, the presence of a strained layer with considerable thickness is possible. To obtain the ~10% magnetization increase at $T_c(H)$ observed in sample $x=0.193$, the width of the interfacial layer outside the CO core is estimated to be ~120 Å if the average size of the CO domains is ~3000 Å. This seems to be reasonable. Unfortunately, an outside layer much thicker than 200–400 Å must be assumed to explain the large magnetization increase in other samples if the same domain size is used. For example, to accommodate the layer thickness to 200–400 Å, a domain size of ~1000 Å should be postulated for $La_{0.67-x}Bi_xCa_{0.33}MnO_3$ ($x=0.167$), in which the magnetization increment at $T_c(H)$ is ~60%. It is obviously smaller than the observed ~2000–5000 Å in a similar compound $La_{0.625-x}Pr_xCa_{0.375}MnO_3$ ($x=0.375$).[18] Though we may argue that cases in $La_{0.67-x}Bi_xCa_{0.33}MnO_3$ could be somewhat different from $La_{0.625-x}Pr_xCa_{0.375}MnO_3$ due to the different properties of Bi and Pr, different sintering conditions and different contents of anionic or cationic vacancies of the two series, which may influence grain size, then possibly domain size of the coexisted phases (it has been reported that the replacement of Cr for Mn can smash the CO domains in $La_{0.325}Ca_{0.675}MnO_3$),[41] a final explanation for the nature of the low-temperature transition based on the present data is difficult, and we would like to leave it to more detailed studies.

(iii) Noting a fact that ~1.7% Cr ions are required to melt the CO phase in the present sample (it occupies ~74% of the total phases), then ~2% Cr may be needed if the sample is composed of a single CO phase. In contrast, to destroy the CO in $Nd_{0.5}Ca_{0.5}MnO_3$, ~0.06 Cr are enough.[30] Therefore, Cr doping is much more effective for the multiphase coexisted compounds. In addition, Cr/Fe affects the CO/FM phase in a manner as if the another phase is not present when the doping level is low, and only the conventional Mn-site doping effects are produced in this case. When the content of dopants is so large that the introduction of these dopants influences the FM-CO competition significantly, a deviation from the conventional doping effects appears. The sharp drop of $T_c(L)$ from ~220 K to ~185 K in the case of Cr doping and from ~200 K to ~120 K for Fe doping are reflections of this process.

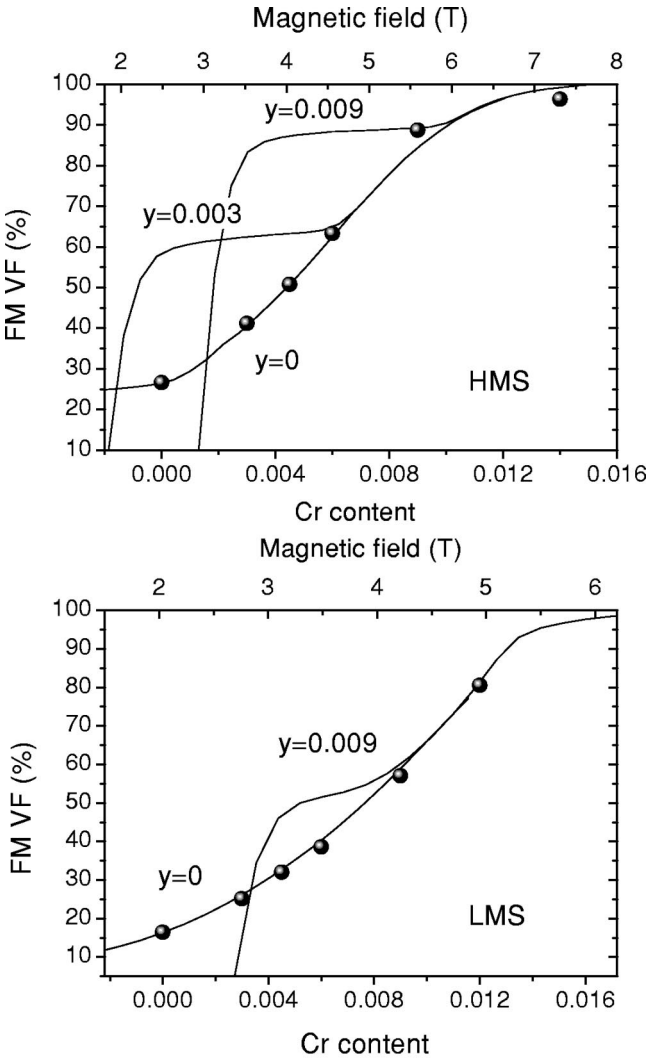

FIG. 12. A comparison of the effects of magnetic field and Cr doping. Solid lines are isothermal magnetization curves after proper zero-point shifts along the horizontal axis. Black circles are results due to Cr doping.

In Fig. 8, the VF of the FM phase as a function of the content of Bi in $La_{0.67-x}Bi_xCa_{0.33}MnO_3$ is also presented. The similarity of the VF(x) and VF(y) curves, even the detailed features, manifests the exactly opposite effects of the Bi doping and the Cr doping. Compared to Bi, however, Cr doping is much more effective, and a simple estimate indicates that 1% increase in Cr is equivalent to ~4.6% decrease in Bi. This observation is consistent with the reports that the effect of the *B*-site doping is much stronger than that of the *A*-site doping. Meanwhile, the deviation of T_c from lattice effects, due to phase separation, can also be amended by Cr doping except for a small extra decrease of T_c (~5 K). Therefore, effects of Bi doping can be counteracted by Cr doping effectively.

Similar to Cr doping, an applied field promotes the development of the FM phase, at the expense of the charge-ordered phase. Shifting the M-H curves of different Cr content in Fig. 7 along the H axis, as shown in Fig. 12, the lifting part of the curves joins each other, forming a smooth

curve that shows the melting process of the charge-ordered phase under magnetic field. It is interesting that all the magnetization corresponding to different Cr doping also collapse into this curve, manifesting the equivalence of Cr doping to magnetic field and the universality of the process of the CO to FM conversion. A simple estimate gives that 1% Cr is equivalent to ~ 4.5 T for the LMS and 6 T for the HMS. Denote the energy difference between the CO and FM states by Δ (per Mn ion), and considering a fact that an applied field depresses this energy by $\sim 0.213\mu_0 H$ (*vide infra*), it is easy to derive that 1% Cr reduces Δ by ~ 0.96 meV.

(iv) The two-step melting of the CO phase with the incorporation of Cr may be universal feature of the complex phase-separated system. The small energy difference between the CO and FM states in $La_{0.67-x}Bi_xCa_{0.33}MnO_3$ is the reason for the simultaneous occurrence of the two competing phases for that, in this case, Δ can be overcome by the energy gained from the random-phase fluctuation. The free energy of a phase-separated system can be simplified as[42]

$$F(X,H) = (\Delta - 0.213\mu_0 H)X - \eta_F X^{1/2} - \eta_{AF}(1-X)^{1/2} + \gamma(0.5 - |1-X|)^{2/3}, \quad (1)$$

where X is the volume fraction of the FM phase, $-0.213\mu_0 H$ is the average Zeeman energy per Mn ion with a moment of $3.67\mu_B$, η_F and η_{AF} are parameters characterizing the phase fluctuation that favors, respectively, the FM and CO AFM states. Effects of domain wall are considered in the last term. Δ can be depressed by doping Cr into Mn site or by applying a magnetic field, and the CO phase transforms into the FM phase when $\Delta - 0.213\mu_0 H \leqslant 0$. Δ may be small in the present compounds considering a fact that a field of ~ 5 T can depress the CO completely. The right inset of Fig. 7 shows the calculated FM VF based on Eq. (1) with the parameters $\Delta = 1$ meV, $\eta_F = 0.96$ meV, $\eta_{AF} = 0.6$ meV, and $\gamma = 0.2$ meV. The FM phase becomes stable when Δ is overcome by Zeeman energy, resulting in a steep jump of VF. The upper kink in the calculated curve for the increasing field branch appears at $H \simeq \Delta/0.213\mu_0$. Its resemblance to the round corner at H_{c2} in the measured curve is evident. It is interesting to note that a full FM alignment is not reached even when $\Delta - 0.213\mu_0 H < 0$, which is obviously a consequence of phase fluctuation. For the present compound, it is obvious that the CO $\rightarrow$ FM conversion begins at H_{c1} and ends at H_{c2}. The observed slow and gradual increase of magnetization with magnetic field is a sign of a broad distribution of Δ, which is clear from the wide H_{c1}-H_{c2} expansion (left inset to Fig. 7). By analogy, the apparent kink in the VF (y) curve may correspond to $\Delta(y) = 0$, while the following long tail from ~ 0.009 to ~ 0.017 for the HMS might be a result of random-phase fluctuation that opposes a homogeneous magnetic state.

V. SUMMARY

Effects of Bi, Cr, and Fe doping on phase separation of $La_{0.67}Ca_{0.33}MnO_3$ have been experimentally studied. As proved by the electron-spin resonance and neutron-diffraction studies, partial replacement of La by Bi causes the simultaneous occurrence of ferromagnetic (FM) phase and charge-ordered antiferromagnetic phase. As a consequence, two subsequent magnetic transitions at ~ 120 K and ~ 230 K are resulted. A strong coupling between the coexisted phases is assumed, which is responsible for the insensitivity of $T_c(L)$, the higher Curie temperature, to Bi doping after the appearance of phase separation, and consistent with the discontinuous variation of $T_c(L)$ with Cr doping. As expected, the substitution of Cr for Mn in this case promotes the FM order, but its effects are significantly different for the two magnetic states. Each Cr drives ~ 100 neighboring unit cells, for the high-moment state, and ~ 60 unit cells, for the low-moment state, into the FM state. Two definite processes can be identified for the melting of the charge-ordered phase. The FM fraction increases rapidly in the initial stage of Cr doping, then slowly when the FM population exceeds $\sim 90\%$. This could be a common feature of the phase-separated system suffering from random phase fluctuation according to a theoretical analysis. Exactly opposite effects on phase constituent are produced by Cr doping and Bi doping, and 1% Cr are equivalent to $\sim 4.6\%$ Bi. In contrast, both Cr doping and magnetic field promote the FM order. 1% Cr correspond to a field of ~ 4.5 T for the low-moment state and 6 T for the high-moment state, reducing the energy difference between the charge-ordered and FM states by ~ 0.96 meV/Mn and ~ 1.3 meV/Mn, respectively.

ACKNOWLEDGMENTS

This work was supported by the Key Project for Elementary Research of China and the National Nature Science Foundation of China.

[1] For a review, see *Colossal Magnetoresistance, Charge ordering, and Related Properties of Manganese Oxides*, edited by C.N.R. Rao and B. Raveau (World Scientific, Singapore, 1998); *Colossal Magnetoresistance Oxides*, edited by Y. Tokura (Gordon and Breach, London, 1999).

[2] P. Schiffer, A.P. Ramirez, W. Bao, and S.-W. Cheong, Phys. Rev. Lett. **75**, 3336 (1995); A.J. Millis, Nature (London) **392**, 147 (1998).

[3] H.Y. Hwang, S.-W. Cheong, P.G. Radaelli, M. Marezio, and B. Batlogg, Phys. Rev. Lett. **75**, 914 (1995).

[4] M.F. Hundely, M. Hawley, R.H. Heffner, O.X. Jia, J.J. Neumeier, J. Tesmer, J.D. Thompson, and X.D. Wu, Appl. Phys. Lett. **67**, 860 (1995).

[5] Z. Jirak, S. Krupicka, Z. Simsa, M. Dlouha, and Z. Vratislav, J. Magn. Magn. Mater. **53**, 153 (1985).

[6] H. Kuwahara, Y. Tomioka, A. Asamitsu, Y. Moritomo, and Y. Tokura, Science **270**, 961 (1995).

[7] A. Asamitsu, Y. Tomioka, and Y. Tokura, Nature (London) **388**, 50 (1997).

[8] T. Kimura, Y. Tomioka, R. Kumai, Y. Okimoto, and Y. Tokura,

Phys. Rev. Lett. **83**, 3940 (1999).
[9] H. Kuwahara, Y. Tomioka, A. Asamitsu, Y. Moritomo, and Y. Tokura, Science **270**, 961 (1995).
[10] Y. Tomioka, A. Asamitsu, H. Kuwahara, and Y. Tokura, Phys. Rev. B **53**, R1689 (1996).
[11] S.-W. Cheong and C. H. Chen, in *Colossal Magnetoresistance, Charge Ordering and Related Properties of Manganese Oxides*, edited by C.N. R. Rao and B. Raveau (World Scientific, Singapore, 1998).
[12] C. Zener, Phys. Rev. **82**, 403 (1951).
[13] P.W. Anderson and H. Hasegawa, Phys. Rev. **100**, 675 (1955).
[14] G.H. Rao, J.R. Sun, J.K. Liang, and W.Y. Zhou, Phys. Rev. B **55**, 3742 (1997).
[15] M.R. Ibarra, G.M. Zhao, J.M. De Teresa, B. Garcia-Landa, Z. Arnold, C. Marquina, P.A. Algarabel, H. Keller, and C. Ritter, Phys. Rev. B **57**, 7446 (1998).
[16] G.H. Rao, J.R. Sun, J.K. Liang, W.Y. Zhou, and X.R. Cheng, Appl. Phys. Lett. **69**, 424 (1996).
[17] J.R. Sun, G.H. Rao, and J.K. Liang, Phys. Status Solidi A **163**, 141 (1997).
[18] M. Uehara, S. Mori, C.H. Chen, and S.-W. Cheong, Nature (London) **399**, 560 (1999).
[19] V. Kiryukhin, B.G. Kim, V. Podzorov, S.-W. Cheong, T.Y. Koo, J.P. Hill, I. Moon, and Y.H. Jeong, Phys. Rev. B **63**, 024420 (2000).
[20] J.A. Souza, R.F. Jardim, R. Muccillo, E.N.S. Muccillo, M.S. Torikachvili, and J.J. Neumeier, J. Appl. Phys. **89**, 6636 (2001).
[21] P.G. Radaelli, R.M. Ibberson, D.N. Argyriou, H. Casalta, K.H. Andersen, S.-W. Cheong, and J.F. Mitchell, Phys. Rev. B **63**, 172419 (2001).
[22] A. Barnabe, A. Maignan, M. Hervieu, F. Damay, C. Martin, and B. Raveau, Appl. Phys. Lett. **71**, 3907 (1997); B. Raveau, A. Maignan, and C. Martin, Solid State Chem. **130**, 162 (1997).
[23] J.R. Sun, G.H. Rao, J.K. Liang, B.G. Shen, and H.K. Wong, Appl. Phys. Lett. **73**, 2998 (1998).
[24] H. Woo, T.A. Tyson, M. Croft, S.-W. Cheong, and J.C. Woicik, Phys. Rev. B **63**, 134412 (2001).
[25] R.A. Young, A. Sakthivel, T.S. Moss, and C.O. Paiva-Santos, J. Appl. Crystallogr. **28**, 366 (1994).
[26] J. Blasco, J. Garcia, J.M. De Teresa, J.M. Ibarra, P.A. Algarabel, and C. Marquina, J. Phys.: Condens. Matter **8**, 7427 (1996).
[27] K.H. Kim, M. Uehara, C. Hess, P.A. Sharma, and S.-W. Cheong, Phys. Rev. Lett. **84**, 2961 (2000).
[28] F. Rivadulla, M. Freita-Alvite, M.A. López-Quintela, L.E. Hueso, D.R. Miguėns, P. Sande, and J. Rivas, J. Appl. Phys. **785**, 91 (2002).
[29] H. Yoshizawa, R. Kajimoto, H. Kawano, Y. Tomioka, and Y. Tokura, Phys. Rev. B **55**, 2729 (1997).
[30] T. Kimura, R. Kumai, Y. Okimoto, Y. Tomioka, and Y. Tokura, Phys. Rev. B **62**, 15021 (2000).
[31] K. Ghosh, S.B. Ogale, R. Ramesh, R.L. Greene, and T. Venkatesan, Phys. Rev. B **59**, 533 (1999).
[32] D. Niebieskikwiat, R.D. Sánchez, and A. Caneiro, J. Magn. Magn. Mater. **237**, 241 (2001).
[33] H. Kuwahara, Y. Tomioka, Y. Moritomo, A. Asamitsu, M. Kasai, R. Kumai, and Y. Tokura, Science **272**, 80 (1996).
[34] V. Podzorov, B.G. Kim, V. Kiryukhin, M.E. Gershenson, and S.-W. Cheong, Phys. Rev. B **64**, 140406 (2001).
[35] W. Prellier, E. Rauwel Buzin, Ch. Simon, B. Mercey, M. Hervieu, S. de Brion, and G. Chouteau, Phys. Rev. B **66**, 024432 (2002).
[36] W. Prellier, Ch. Simon, A.M. Haghiri-Gosnet, B. Mercey, and B. Raveau, Phys. Rev. B **62**, R16337 (2000).
[37] W. Prellier, A.M. Haghiri-Gosnet, B. Mercey, Ph. Lecoeur, M. Hervieu, Ch. Simon, and B. Raveau, Appl. Phys. Lett. **77**, 1023 (2000).
[38] W. Prellier, A. Biswas, M. Rajeswari, T. Venkatesan, and R.L. Greene, Appl. Phys. Lett. **75**, 397 (1999).
[39] R. Mahendiran, B. Raveau, M. Hervieu, C. Michel, and A. Maignan, Phys. Rev. B **64**, 064424 (2001).
[40] R.A. Rao, D. Lavric, T.K. Nath, and C.B. Eoma, L. Wu, and F. Tsui, Appl. Phys. Lett. **73**, 3294 (1998).
[41] T. Katsufuji, S.-W. Cheong, S. Mori, and C.H. Chen, J. Phys. Soc. Jpn. **68**, 1090 (1999).
[42] D.F. Niebieskikwiat, R.D. Sánchez, A. Caneiro, and B. Alascio, Phys. Rev. B **63**, 212402 (2001).